STUDY OF SEALED LEAD/ACID CELLS

J. MRHA*, J. JINDRA and M. MUSILOVÁ

J. Heyrovský Institute of Physical Chemistry and Electrochemistry, Czechoslovak Academy of Sciences, 182 23 Prague 8 (Czechoslovakia)

B. I. TSENTER, I. A. AGUF and R. V. MUSTAFFIN

Accumulator Institute 'Istochnik', 197 137 Leningrad (U.S.S.R.)

(Received April 4, 1990)

Summary

Based on barodynamic characteristics, both the oxygen pressure and the oxygen reduction current at the negative electrode in a sealed lead/acid cell were followed. These data together with potentiodynamic characteristics were used to characterize the time course of the oxygen cycle and its efficiency. Data about the partial pressure of hydrogen were also obtained and experimentally verified. Calculations were made on the assumption that at the positive electrode only oxygen is evolved and at the negative electrode only hydrogen evolution and oxygen reduction proceed.

Introduction

In connection with increasing production of valve-regulated (so-called maintenance-free) lead/acid cells, many authors deal with the determination of the efficiency of the oxygen cycle, which is related with the internal pressure formed in these cells. In our review article [1], this oxygen cycle was discussed from various points of view and the most common methods for the determination of its efficiency were described. Besides the less accurate gravimetric method used earlier, volumetric methods are increasingly used nowadays. These include measurements of the volume and composition of the gas in the sealed cell, or measurements of the internal pressure.

The first volumetric method is based on gas sampling through an outlet stopcock [2 - 6]. The efficiency of the oxygen cycle η_{OC} can be calculated from the equation [4]

$$\eta_{OC} = \left(1 - \frac{I_O}{I}\right) \times 100\ (\%) \tag{1}$$

*Author to whom correspondence should be addressed.

0378-7753/90/$3.50

where I_O denotes the current calculated from the oxygen content in the gas sample and I the overcharging current. The latter corresponds to the generation of oxygen ($I = I^{O_2}$) which is assumed to be the only faradaic process at the positive electrode.

If analytical data about the content of hydrogen are available, the efficiency of the oxygen cycle can be determined from the equation [5, 6]

$$\eta_{OC} = \left(1 - \frac{I_H}{I}\right) \times 100\ (\%) \tag{2}$$

where I_H is the current calculated from the content of hydrogen in the sample; it is equal to the difference between the currents of H_2 evolution and ionization, *i.e.* $I = I^{H_2} - I_{H_2} = I^{H2}$ [7]. The results from both eqns. (1) and (2) are identical within experimental error, which is apparent from the following considerations.

The balance of oxygen expresses that the current corresponding to the oxygen content in the cell, I_O, is equal to the difference between the overcharging current ($I = I^{O_2}$) and the current of oxygen reduction, I_{O_2}

$$I_O = I^{O_2} - I_{O_2} \tag{3}$$

The current balance during overcharge is given as

$$I = I^{O_2} = I_{O_2} + I_H = I_{O_2} + I^{H_2} \tag{4}$$

where I^{H_2} is the current of hydrogen evolution at the negative lead electrode. On eliminating I_H from eqns. (2) and (4) and assuming $I = I^{O_2}$ we obtain

$$\eta_{OC} = \frac{I_{O_2}}{I^{O_2}} \times 100\ (\%) \tag{5}$$

On the other hand, introducing eqn. (3) into eqn. (1) on the same assumption we obtain again eqn. (5).

The efficiency of the oxygen cycle obtained in the described manner attains 98 - 99.5% in optimum cases (valve-regulated cells with electrolyte fixed in a glass microfibre mat with controlled charging voltage or with galvanostatic overcharge at approximately 100 h charging rate).

The second volumetric method consists of the measurement of pressure and analysis of the gas inside the sealed cell, *i.e.*, without gas sampling [8, 9]. The efficiency of the oxygen cycle is calculated from eqn. (5); the method of calculation of the oxygen reduction current from pressure and analytical data was described earlier [10]. The values of η_{OC} thus obtained for optimized cells are also in the range given above. In this way, the influence of various technological factors (electrolyte dosing, overcharge rate, grid alloys, auxiliary electrode, etc.) on the values of η_{OC} was evaluated. The advantage of the method is that it also takes into account the cathodic current corresponding to the eventual reduction

$$PbSO_4 + 2e^- + H^+ \longrightarrow Pb + HSO_4^- \quad (6)$$

in addition to the reduction of oxygen and evolution of hydrogen.

Another method for the determination of the efficiency of the oxygen cycle from eqn. (5) uses a built-in oxygen electrode for reduction of oxygen in the sealed system to determine the oxygen reduction current [11].

Besides the methods based on eqn. (5), it is possible to determine the oxygen reduction rate at the negative electrode of flooded sealed lead/acid cells by using auxiliary catalytic electrodes operating in an optimum potential region. Thus, the volume of oxygen reduced at the lead electrode per unit time (in ml cm^{-2} h^{-1}) is determined practically in the absence of overpressure [12, 13].

Another method for the determination of the oxygen reduction rate consists of mathematical analysis of the pressure increase during overcharge and of the pressure decay during idling immediately after overcharge [14]. The pressure variations are caused by corrosion phenomena especially in more concentrated solutions of H_2SO_4 (K), gas evolution at the electrodes during overcharge (L), and reduction rate of oxygen (R). Thus,

$$\text{pressure increase (on charging)} = K + L - R \ (\text{kPa h}^{-1}) \quad (7)$$

$$\text{pressure decay (on idling)} = R - K \ (\text{kPa h}^{-1}) \quad (8)$$

The pressure increase corresponding to corrosion phenomena, K, is determined during long-term idling of the sealed cell, and then the oxygen reduction rate, R, is found from the latter equation (this value is preferably referred to a unit current).

Some authors recommend the determination of the so-called kinetic constant of oxygen reduction, Z [15]. This is found from the time dependence of the pressure at the lead electrode drawn out from the electrolyte after charging and placed in a closed cell filled with air.

The present work deals with the determination of the efficiency of the oxygen cycle according to eqn. (5) by using the second volumetric method (further: barodynamic method) but without analytical data for the content of O_2 and H_2 in the gas phase of the cell on the assumption that reaction (6) can be neglected.

Experimental

Barodynamic and potentiodynamic curves were measured for various charging currents in a specially designed cylindrical test cell made of organic glass. The cell was provided with a lid which could be hermetically closed by means of four clamps. The electrode system included one positive and two

negative working electrodes and a PbO_2 reference electrode. The electrodes were separated by a glass fibre separator and provided with lead current leads passing through the lid. The electrode system was compressed by plastic spacers. To minimize the dead space of the cell, the electrode system was placed between two organic glass segments. A pressure sensor and a stopcock serving as gas outlet or inlet were placed on the lid.

The electrodes were dry charged, their dimensions were 80 × 50 × 2 mm and the grids were made of pure lead. The nominal capacity of the positive electrodes was about 2.4 A h.

The glass separator FS 972 (Binzer, F.R.G.) was 2.2 mm in thickness, its square density was 285 g/m^2, the content of binder 2%, porosity 92% and effective pore diameter 1 - 8 μm; it covered all working electrodes. Before assembling the cell, the electrodes and the separator layers were wetted with electrolyte (H_2SO_4 of density 1.28 g cm^{-3} containing 22 g per litre of concentrated H_3PO_4). The total electrolyte content in the cell was 45 g. The tightness of the closed cell was checked by filling with nitrogen at an overpressure of 300 kPa. The gas space of the cell was determined volumetrically with a nitrogen gas burette as 34.3 cm^3. The measurements were made at 25 °C. Charging, overcharging and discharging of the cell proceeded in the galvanostatic regime.

Results and discussion

Basic considerations

The method for evaluation of the barodynamic curves was proposed at the beginning of the eighties for sealed Ni/Cd cells [16] and it is based on the combination of Faraday's law for the charging process with the equation of state of ideal gases

$$It = mzF \tag{9}$$

$$PV = mRT \tag{10}$$

where I denotes overcharging current, t time of overcharging, m quantity of gas in moles, z charge number of the reaction, P pressure inside the cell, and V volume of the gas space in the cell. On combining these laws we obtain eqn. (11)

$$\frac{P}{t} = \frac{RT}{FV}\frac{I}{z} \tag{11}$$

which can also be written in the differential form

$$\frac{dP}{dt} = \frac{\alpha_0}{z} I \tag{12}$$

where $\alpha_0 = RT/FV$ is a cell constant.

The method described was used by us for sealed lead/acid laboratory cells. For the evolution and reduction of oxygen, we have $z = 4$, for the evolution of hydrogen $z = 2$, and from eqn. (12) it follows that

$$\frac{dP}{dt} = \frac{1}{4}\alpha_0 I^{O_2} + \frac{1}{2}\alpha_0 I^{H_2} - \frac{1}{4}\alpha_0 I_{O_2} \tag{13}$$

where P denotes total pressure of the gas mixture in the system, I^{O_2} and I^{H_2} are the currents due to evolution of the gases, and I_{O_2} is the reduction current of oxygen. The latter quantity must be distinguished from I_O in eqns. (1) and (3) which is determined from the gas analysis, whereas the value of I_{O_2} is found from eqn. (13) as shown in our preceding work [17], where the necessary values of I^{H_2} were obtained from measurements of cathodic polarization of a fully charged negative Pb electrode. The results were evaluated in the form of the Tafel equation

$$E_{(-)} = a + b \log I^{H_2} \tag{14}$$

The values of I^{H_2} obtained from polarization curves for the Pb electrode were subject to errors due to scatter of the experimental points; therefore the method used in ref. 17 was modified in the present work by using the current balance (4) instead of eqn. (14). It should be noted that the symbol I_H used for the hydrogen evolution current in eqn. (2) and in refs. 4 - 6 is replaced by I^{H_2} beginning from eqn. (13).

On eliminating I^{H_2} from eqns. (13) and (4) we obtain

$$\frac{dP}{dt} = \frac{3}{4}\alpha_0(I - I_{O_2}) \tag{15}$$

whence it follows for the oxygen reduction current

$$I_{O_2} = I - \frac{4}{3\alpha_0}\frac{dP}{dt} \tag{16}$$

and the hydrogen evolution current is obtained from eqns. (4) and (16) in the form

$$I^{H_2} = \frac{4}{3\alpha_0}\frac{dP}{dt} \tag{17}$$

On eliminating I_{O_2} from eqns. (5) and (16) we obtain for the efficiency of the oxygen cycle

$$\eta_{OC} = 1 - \frac{4}{3\alpha_0}\frac{dP}{dt} \tag{18}$$

Experimental data and their evaluation

In Fig. 1 the potentiodynamic characteristics of the cell electrodes and the barodynamic characteristics obtained during galvanostatic charging and overcharging of an initially discharged cell at various currents are shown. The potentiodynamic curves of the positive electrode (Fig. 1(a)) show that the

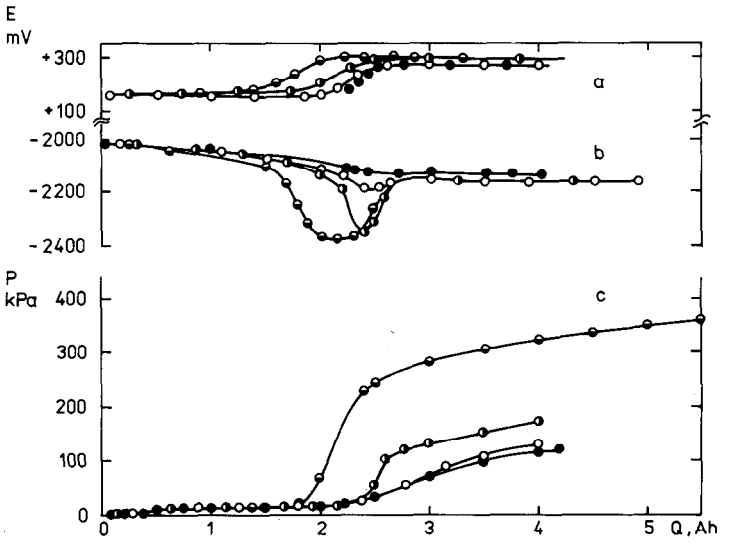

Fig. 1. Potentiodynamic (a, b) and barodynamic (c) curves for a model sealed lead/acid cell. Charging current (mA): ● 200; ○ 300; ◑ 400; ⊖ 500.

potential is constant during the period corresponding to the oxidation of $PbSO_4$. After supplying 60 - 90% of the full charge (2.4 A h represents 100%) the potential begins to shift towards more positive values and at the same time the oxygen evolution starts. The higher the current the sooner this appears. The potential eventually reaches a constant value corresponding to the evolution of oxygen.

The potentiodynamic curves of the negative electrode (Fig. 1(b)) show, in contrast to the positive, a gradual potential shift to more cathodic values during reduction of $PbSO_4$ (eqn. (6)); and this is followed by a more rapid shift related to the evolution of hydrogen. After reaching a cathodic minimum, the potential returns to more anodic values during overcharge, and eventually reaches a constant value (the depolarization of a negative electrode with oxygen). The electrode potential is apparently related to the reduction of oxygen at the negative electrode; this process starts as soon as the oxygen pressure at the Pb electrode attains a sufficiently high value. The minimum is broader at higher current, since the evolution of hydrogen sets in sooner.

It can be seen from the barodynamic curves in Fig. 1(c) that after charging to about 15% of the cell capacity the pressure rises slightly, which is probably due to the formation of some oxygen at the positive electrode; and the reduction of oxygen at the negative electrode sets in. The oxygen evolution at this initial stage is probably caused by electrolyte deficiency (the cell contains much less electrolyte than usual in vented cells). The positive electrode behaves similarly to that in a Ni/Cd accumulator.

After charging to 75 - 95% of the discharge capacity there is a pronounced increase of the pressure. The higher the current the sooner this

occurs. However, after charging to 100 - 105%, the further pressure increase becomes less pronounced, since the content of oxygen in the cell is so high that its reduction at the negative electrode becomes sufficiently rapid; the oxygen cycle starts to operate fully. This causes the potential of the Pb electrode to attain a steady value (Fig. 1(b)). During long-term overcharge, the rate of the pressure increase becomes constant, the efficiency of the oxygen cycle does not rise any more and attains its maximum (compare eqn. (18)).

Figure 2 illustrates the course of the calculated oxygen pressure during charging and overcharging a discharged cell at various currents. The oxygen partial pressure was calculated from the total pressure (P, Fig. 1) and the partial pressure of hydrogen given as

$$\Delta P_{H_2} = \frac{\alpha_0}{2} I^{H_2} \Delta t \tag{19}$$

Thus, the oxygen partial pressure is given as

$$\Delta P_{O_2} = \Delta P - \frac{\alpha_0}{2} I^{H_2} \Delta t \tag{20}$$

On combining eqns. (17) and (20) we obtain

$$P_{O_2} = P - \frac{2}{3} \frac{dP}{dt} = \frac{1}{3} \Delta P \tag{21}$$

It is apparent from Fig. 2 that the mentioned slight pressure increase after supplying about 15% of the full charge indeed corresponds to oxygen formed at the positive electrode. Nearly constant oxygen pressure up to supplying 75 - 95% of the full charge substantiates the assumption about the reduction of oxygen at the negative electrode.

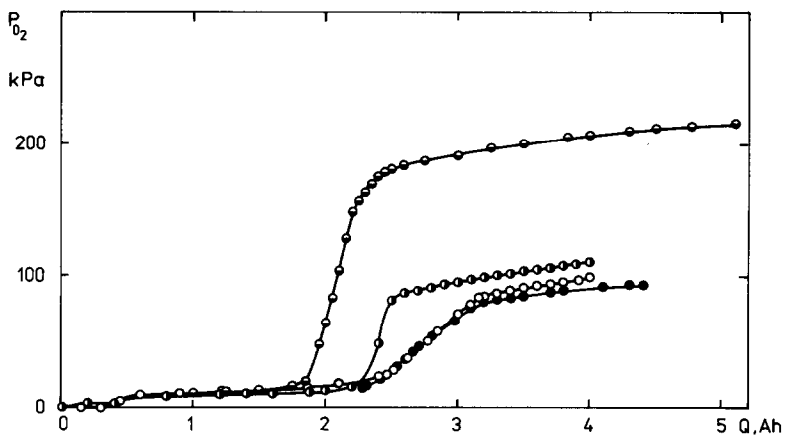

Fig. 2. Calculated partial pressure of oxygen in a model sealed lead/acid cell during galvanostatic charging at various currents. For labels of the curves see Fig. 1.

After supplying 75 - 95% of the full charge, the internal pressure markedly increases (Figs. 1 and 2), evidence for the almost simultaneous formation of hydrogen and oxygen. By comparing the right-hand portions of the curves in Figs. 1 and 2 it follows that the partial pressure of oxygen increases only very little during full operation of the oxygen cycle and that the increase of the total pressure (cf. Fig. 1) during this period is caused mainly by hydrogen.

The validity of the calculation of the partial pressure of hydrogen can be verified by comparison of the calculated values with the measured ones. These were obtained by measuring the steady pressure about 16 h after interrupting the overcharge, *i.e.*, in a situation where practically all oxygen was reduced at the negative electrode. The results obtained at various currents are compared in Table 1, whence if follows that the maximum difference between the two values amounts to 7 - 8%, which is within the limits of experimental errors.

TABLE 1

Comparison of calculated and measured values of the partial pressure of hydrogen in a sealed accumulator at various currents

Charging current (mA)	Partial pressure (kPa)	
	Calculated	Measured
200	28	27.3
300	32	31
400	62	57
500	150	139

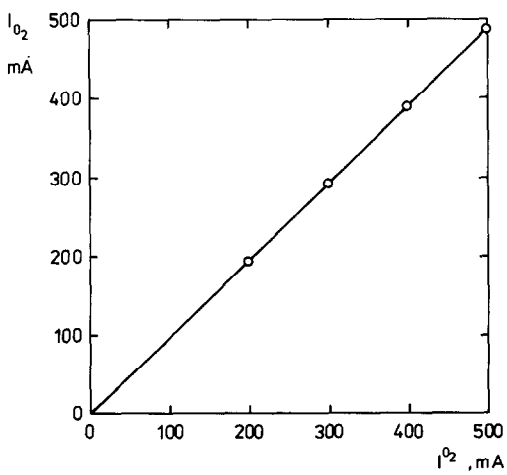

Fig. 3. Dependence of the oxygen reduction current, I_{O_2}, on the oxygen evolution current, I^{O_2}, at various charging currents. Situation at the end of charging.

Figure 3 illustrates the calculated dependence of the oxygen reduction current, I_{O_2}, on the overcharge current toward the end of the overcharging period ($I = I^{O_2}$). The dependence is linear in accord with eqn. (5) and its slope gives the efficiency of the oxygen cycle, η_{OC}, in our case 99%. This is in accord with the results published earlier [18], suggesting that practically no hydrogen is formed at the negative electrode at the end of charging.

Conclusions

(i) Based on current and oxygen balances in a sealed lead/acid cell, a method is proposed for the calculation of the oxygen partial pressure and the oxygen reduction current from barodynamic curves measured during galvanostatic charge and overcharge.

(ii) Information about electrochemical processes leading to the formation of oxygen and hydrogen and reduction of oxygen were obtained from the calculated oxygen partial pressure and potentiodynamic characteristics of the negative and positive electrodes.

(iii) The efficiency of the oxygen cycle was calculated from the calculated oxygen reduction current during the overcharge period. For example, it attained 99% after long-term overcharge (230% of the discharge capacity).

(iv) The calculated partial pressure of hydrogen was in good agreement with the value measured after a prolonged overcharge, evidence that the method of calculation is justified.

References

1 J. Mrha, K. Micka, J. Jindra and M. Musilová, *J. Power Sources, 27* (1989) 91.
2 K. R. Bullock and E. C. Laird, *J. Electrochem. Soc., 129* (1982) 1393.
3 B. L. McKinney, B. K. Mahato and K. R. Bullock, in K. R. Bullock and D. Pavlov (eds.), *Advances in Lead-Acid Batteries,* Proc. Vol. 84-14, Battery Division, The Electrochemical Society, Pennington, NJ, 1984, p. 426.
4 J. S. Symanski, B. K. Mahato and K. R. Bullock, *J. Electrochem. Soc., 135* (1988) 548.
5 A. I. Harrison and B. A. Wittey, in L. J. Pearce (ed.), *Power Sources 10,* Taylor and Francis, Basingstoke, U.K., 1984, p. 447.
6 A. I. Harrison, *Chem. Ind., 6* (1986) 201.
7 I. A. Aguf, N. K. Grigalyuk, O. Z. Rasima and T. P. Chizhik, *Elektrokhimiya, 24* (1988) 414.
8 H. Dietz, M. Radwan, J. Garche, H. Doering and K. Wiesener, *J. Power Sources, 30* (1990) 381.
9 H. Dietz, S. Voss, H. Doering, J. Garche and K. Wiesener, *J. Power Sources,* in press.
10 J. Garche, D. Ohms, H. Dietz, Nguyen Duc Hung, K. Wiesener and J. Mrha, *Electrochim. Acta, 34* (1989) 1603.
11 E. A. Khomskaya, N. F. Gorbacheva, T. V. Arkhipova and N. F. Burfanova, *Elektrokhimiya, 21* (1985) 363.
12 I. Nikolov, G. Papazov, V. Naidenov, T. Vitanov and D. Pavlov, *Abstr., Int. Conf. Lead/Acid Batteries, LABAT '89, Drujba, Varna, Bulgaria, 1989,* Abstr. No. 48.

13 G. Papazov, I. Nikolov, M. Bojinov, D. Pavlov and T. Vitanov, *Abstr., Int. Conf. Lead/Acid Batteries, LABAT '89, Drujba, Varna, Bulgaria, 1989*, Abstr. No. 49.
14 J. Mrha, U. Vogel, S. Kreuels and W. Vielstich, *J. Power Sources, 27* (1989) 201.
15 M. Maja and N. Penazzi, *J. Power Sources, 22* (1988) 1.
16 B. J. Tsenter, R. V. Boldin and L. M. Levinson, *Zh. Prikl. Khim., 54* (1981) 1861.
17 B. J. Tsenter, R. V. Mustaffin, J. Mrha, J. Jindra and M. Musilová, *Zh. Prikl. Khim., 63* (1990) 692.
18 J. G. Chirkov, E. A. Khomskaya and V. V. Pechenkin, *Sb. Isled. v Obl. Prikl. Elektrohim., Izd. Saratov. Gosud. Univ.*, 1984, p. 13.